EUROPEAN ORGANIZATION FOR NUCLEAR RESEARCH

CERN-PPE/97-118
29 August 1997

# The Spin-Dependent Structure Function $g_1(x)$ of the Proton from Polarized Deep-Inelastic Muon Scattering

*The Spin Muon Collaboration (SMC)*

## Abstract

We present a new measurement of the virtual photon proton asymmetry $A_1^{\rm p}$ from deep inelastic scattering of polarized muons on polarized protons in the kinematic range $0.0008 < x < 0.7$ and $0.2 < Q^2 < 100$ GeV$^2$. With this, the statistical uncertainty of our measurement has improved by a factor of 2 compared to our previous measurements. The spin-dependent structure function $g_1^{\rm p}$ is determined for the data with $Q^2 > 1$ GeV$^2$. A perturbative QCD evolution in next-to-leading order is used to determine $g_1^{\rm p}(x)$ at a constant $Q^2$. At $Q^2 = 10$ GeV$^2$ we find, in the measured range, $\int_{0.003}^{0.7} g_1^{\rm p}(x){\rm d}x = 0.139 \pm 0.006$ (stat) $\pm 0.008$ (syst) $\pm 0.006$ (evol). The value of the first moment $\Gamma_1^{\rm p} = \int_0^1 g_1^{\rm p}(x){\rm d}x$ of $g_1^{\rm p}$ depends on the approach used to describe the behaviour of $g_1^{\rm p}$ at low $x$. We find that the Ellis-Jaffe sum rule is violated. With our published result for $\Gamma_1^{\rm d}$ we confirm the Bjorken sum rule with an accuracy of $\approx 15\%$ at the one standard deviation level.

*Accepted for Publication in Physics Letters B*

B. Adeva[18], E. Arik[2], A. Arvidson[21,a], B. Badelek[21,23], G. Bardin[17,†], G. Baum[1], P. Berglund[8], L. Betev[13], R. Birsa[20], N. de Botton[17], F. Bradamante[20], A. Bravar[11], A. Bressan[20], S. Bültmann[1,b], E. Burtin[17], D. Crabb[22], J. Cranshaw[20,c], T. Çuhadar[2], S. Dalla Torre[20], R. van Dantzig[15], B. Derro[4], A. Deshpande[24], S. Dhawan[24], C. Dulya[15,4,d], S. Eichblatt[5,e], D. Fasching[16,f], F. Feinstein[17], C. Fernandez[18,9], S. Forthmann[7], B. Frois[17], A. Gallas[18], J.A. Garzon[18,9], H. Gilly[6], M. Giorgi[20], S. Goertz[3], G. Gracia[18,g], N. de Groot[15,h], K. Haft[13], D. von Harrach[11], T. Hasegawa[14,i], P. Hautle[5,j], N. Hayashi[14,k], C.A. Heusch[5,l], N. Horikawa[14], V.W. Hughes[24], G. Igo[4], S. Ishimoto[14,m], T. Iwata[14], E.M. Kabuß[11], T. Kageya[14], A. Karev[10], T.J. Ketel[15], J. Kiryluk[23], Yu. Kisselev[10], V. Krivokhijine[10], W. Kröger[5,l], V. Kuktin[10], K. Kurek[23], J. Kyynäräinen[1,8], M. Lamanna[20], U. Landgraf[6], J.M. Le Goff[17], F. Lehar[17], A. de Lesquen[17], J. Lichtenstadt[19], M. Litmaath[15,n], A. Magnon[17], G.K. Mallot[11], F. Marie[17], A. Martin[20], J. Martino[17], T. Matsuda[14,i], B. Mayes[9], J.S. McCarthy[22], K. Medved[10], W. Meyer[3], G. van Middelkoop[15], D. Miller[16], Y. Miyachi[14], K. Mori[14], J. Moromisato[5,o], J. Nassalski[23], L. Naumann[5,†], T.O. Niinikoski[5], J.E.J. Oberski[15], A. Ogawa[14,p], M. Perdekamp[24], H. Pereira[17], F. Perrot-Kunne[17], D. Peshekhonov[10], L. Pinsky[9], S. Platchkov[17], M. Plo[18], D. Pose[10], H. Postma[15], J. Pretz[11], R. Puntaferro[20], G. Rädel[5], A. Rijllart[5], G. Reicherz[3], M. Rodriguez[21,q], E. Rondio[23,5], B. Roscherr[24], I. Sabo[19], J. Saborido[18], A. Sandacz[23], I. Savin[10], P. Schiavon[20], A. Schiller[7], E. P. Sichtermann[15], F. Simeoni[20], G.I. Smirnov[10], A. Staude[13], A. Steinmetz[11,r], U. Stiegler[5], H. Stuhrmann[7], M. Szleper[23], F. Tessarotto[20], D. Thers[17], W. Tlaczala[23,s], A. Tripet[1], G. Unel[2], M. Velasco[16,n], J. Vogt[13], R. Voss[5], C. Whitten[4], R. Windmolders[12], W. Wislicki[23], A. Witzmann[6,t], J. Ylöstalo[8], A.M. Zanetti[20], K. Zaremba[23,s]

[1] University of Bielefeld, Physics Department, 33501 Bielefeld, Germany[aaa]
[2] Bogaziçi University and Istanbul Technical University, Istanbul, Turkey[bbb]
[3] University of Bochum, Physics Department, 44780 Bochum, Germany[aaa]
[4] University of California, Department of Physics, Los Angeles, 90024 CA, USA[ccc]
[5] CERN, 1211 Geneva 23, Switzerland
[6] University of Freiburg, Physics Department, 79104 Freiburg, Germany[aaa]
[7] GKSS, 21494 Geesthacht, Germany[aaa]
[8] Helsinki University of Technology, Low Temperature Laboratory and Institute of Particle Physics Technology, Espoo, Finland
[9] University of Houston, Department of Physics, Houston, 77204-5506 TX, USA[ccc,ddd]
[10] JINR, Dubna, RU-141980 Dubna, Russia
[11] University of Mainz, Institute for Nuclear Physics, 55099 Mainz, Germany[aaa]
[12] University of Mons, Faculty of Science, 7000 Mons, Belgium
[13] University of Munich, Physics Department, 80799 Munich, Germany[aaa]
[14] Nagoya University, CIRSE and Department of Physics, Furo-Cho, Chikusa-Ku, 464 Nagoya, Japan[eee]
[15] NIKHEF, Delft University of Technology, FOM and Free University, 1009 AJ Amsterdam, The Netherlands[fff]
[16] Northwestern University, Department of Physics, Evanston, 60208 IL, USA[ccc,ddd]
[17] C.E.A. Saclay, DAPNIA, 91191 Gif-sur-Yvette, France[ggg]
[18] University of Santiago, Department of Particle Physics, 15706 Santiago de Compostela, Spain[hhh]
[19] Tel Aviv University, School of Physics, 69978 Tel Aviv, Israel[iii]
[20] INFN Trieste and University of Trieste, Department of Physics, 34127 Trieste, Italy
[21] Uppsala University, Department of Radiation Sciences, 75121 Uppsala, Sweden
[22] University of Virginia, Department of Physics, Charlottesville, 22901 VA, USA[ccc]
[23] Soltan Institute for Nuclear Studies and Warsaw University, 00681 Warsaw, Poland[jjj]
[24] Yale University, Department of Physics, New Haven, 06511 CT, USA[ccc]
[a] Now at Gammadata, Uppsala, Sweden
[b] Now at University of Virginia, Department of Physics, Charlottesville, 22901 VA, USA[ccc]
[c] Now at INFN Trieste, 34127 Trieste, Italy
[d] Now at CIEMAT, Avda Complutense 22, 28040, Madrid, Spain
[e] Now at Fermi National Accelerator Laboratory, Batavia, 60510 IL, USA
[f] Now at University of Wisconsin, USA
[g] Now at NIKHEF P.O.B. 41882, 1009 DB Amsterdam, The Netherlands
[h] Now at SLAC, Stanford 94309 CA USA
[i] Permanent address: Miyazaki University, Faculty of Engineering, 889-21 Miyazaki-Shi, Japan
[j] Permanent address: Paul Scherrer Institut, 5232 Villigen, Switzerland
[k] Permanent address: The Institute of Physical and Chemical Research (RIKEN), wako 351-01, Japan
[l] Permanent address: University of California, Institute of Particle Physics, Santa Cruz, 95064 CA, USA
[m] Permanent address: KEK, Tsukuba-Shi, 305 Ibaraki-Ken,Japan
[n] Now at CERN, 1211 Geneva 23, Switzerland
[o] Permanent address: Northeastern University, Department of Physics, Boston, 02115 MA, USA
[p] Now at Penn. State University, 303 Osmond Lab, University Park, 16802 PA, USA
[q] Permanent address: University of Buenos Aires, Physics Department, 1428 Buenos Aires, Argentina
[r] Now at University of Munich, Physics Department, 80799 Munich, Germany
[s] Permanent address: Warsaw University of Technology, Warsaw, Poland

Polarized deep inelastic lepton-nucleon scattering is an important tool to study the internal spin structure of the nucleon. Measurements on proton, deuteron and neutron targets allow verification of the Bjorken sum rule [1] which is a fundamental relation of QCD. The improved accuracy of data collected by experiments at CERN and SLAC in the past few years has motivated and allowed perturbative QCD analyses of the nucleon spin-dependent structure function $g_1(x, Q^2)$ at next-to-leading-order (NLO) [2, 3, 4].

In this paper, we report on a new measurement of the virtual photon proton asymmetry $A_1^{\rm p}$ by the Spin Muon Collaboration (SMC), obtained by scattering longitudinally polarized muons of approximately 190 GeV energy on longitudinally polarized protons in the kinematic range $0.0008 < x < 0.7$ and $0.2\ {\rm GeV}^2 < Q^2 < 100\ {\rm GeV}^2$. The data were collected in 1996 with the high-energy muon beam M2 of the CERN SPS using solid ammonia as the polarized target material. They complement earlier data taken in 1993 at the same beam energy using butanol as the target material [5, 6]. The statistical precision of the combined $A_1^{\rm p}$ data sets is a factor of approximately two improved compared to our 1993 data. Using the data with $Q^2 > 1\ {\rm GeV}^2$ and $x > 0.003$ we determine the spin structure function $g_1$ of the proton. In this paper we present the new data and give a brief description of the analysis. In Ref. [6] we have given a detailed description of the method of the measurement and data analysis for the determination of the spin structure function of the proton.

The cross section asymmetry for parallel and antiparallel configurations of longitudinal beam and target polarizations is given by

$$A_{\parallel}^{\rm p} = \frac{\sigma^{\uparrow\downarrow} - \sigma^{\uparrow\uparrow}}{\sigma^{\uparrow\downarrow} + \sigma^{\uparrow\uparrow}} \ . \tag{1}$$

The evaluation of the asymmetry $A_{\parallel}^{\rm p}$ requires knowledge of the incident muon and target proton polarizations, and of the dilution factor which accounts for the fact that only a fraction of the target nucleons is polarized. The beam polarization was determined by measuring the cross section asymmetry for the scattering of polarized muons on polarized atomic electrons [6, 7]. For the average muon energy of 188 GeV, the polarization is $P_\mu = -0.77 \pm 0.03$. The energy dependence of the polarization is taken into account event by event.

The choice of ammonia as the target material rather than butanol which was used in our 1993 measurement [5, 6], increased the dilution factor by $\approx 30\%$. The average longitudinal proton polarization over the entire data taking period was $P_{\rm p} = \pm 0.89$, known with an overall accuracy $\Delta P_{\rm p}/P_{\rm p} = 2.7\%$. The polarization, $P_{\rm N}$, of the $^{14}$N nuclei was


[t)] Now at F.Hoffmann-La Roche Ltd., CH-4070 Basel, Switzerland


[aaa)] Supported by the Bundesministerium für Bildung, Wissenschaft, Forschung und Technologie
[bbb)] Partially supported by TUBITAK and the Centre for Turkish-Balkan Physics Research and Application (Bogaziçi University)
[ccc)] Supported by the U.S. Department of Energy
[ddd)] Supported by the U.S. National Science Foundation
[eee)] Supported by Monbusho Grant-in-Aid for Scientific Research (International Scientific Research Program and Specially Promoted Research)
[fff)] Supported by the National Science Foundation (NWO) of The Netherlands
[ggg)] Supported by the Commissariat à l'Energie Atomique
[hhh)] Supported by Comision Interministerial de Ciencia y Tecnologia
[iii)] Supported by the Israel Science Foundation.
[jjj)] Supported by KBN SPUB/P3/209/94 and /P3/21/97


[†)] Deceased.

determined [8] with an accuracy $\Delta P_{\rm N}/P_{\rm N}$ of better than 10% in dedicated measurements. Its value was found to relate to the proton polarization as predicted by the equilibrium spin temperature relation [9]. In the analysis the nitrogen polarization was calculated from the measured proton polarization using that relation. The typical nitrogen polarization was $P_{\rm N} = \pm 0.14$.

The asymmetry $A_{\parallel}^{\rm p}$ and the spin-dependent structure function $g_1^{\rm p}$ are related to the virtual photon proton asymmetries $A_1^{\rm p}$ and $A_2^{\rm p}$ [10, 11] by

$$A_{\parallel}^{\rm p} = D(A_1^{\rm p} + \eta A_2^{\rm p}), \qquad\qquad g_1^{\rm p} = \frac{F_2^{\rm p}}{2x(1+R)}(A_1^{\rm p} + \gamma A_2^{\rm p}), \tag{2}$$

in which the factors $\eta$ and $\gamma$ depend only on kinematic variables; the depolarization factor $D$ depends, in addition, on the ratio of total photoabsorption cross sections for longitudinally and transversely polarized virtual photons $R = \sigma_{\rm L}/\sigma_{\rm T}$. The virtual photon proton asymmetries are defined as

$$A_1^{\rm p} = \frac{\sigma_{1/2} - \sigma_{3/2}}{\sigma_{1/2} + \sigma_{3/2}}, \qquad\qquad A_2^{\rm p} = \frac{2\sigma^{\rm TL}}{\sigma_{1/2} + \sigma_{3/2}}, \tag{3}$$

where $\sigma_{1/2}$ ($\sigma_{3/2}$) is the total photoabsorption cross section of a transverse virtual photon by a proton, with total spin projection 1/2 (3/2) in the photon direction, and $\sigma^{\rm TL}$ is a term arising from the interference between transverse and longitudinal amplitudes.

In the kinematic region of our measurement $\eta$ and $\gamma$ are small and $A_2^{\rm p}$ was measured and found to be consistent with zero. We therefore neglect the terms proportional to $A_2^{\rm p}$ in Eq. (2). The systematic uncertainty due to a possible residual contribution from $A_2^{\rm p}$ is estimated using the SMC [12] and the SLAC E143 [13] measurements. The E143 results have better statistical accuracy but do not extend to low $x$. Assuming that $A_2^{\rm p}\sqrt{Q^2}$ is $Q^2$ independent, the E143 measurements are evaluated at the $Q^2$ of SMC data in each $x$ bin. The combined $A_2^{\rm p}$ data are then parametrized and the parametrization is used in the estimation of the systematic uncertainty .

When calculating $A_{\parallel}^{\rm p}$ we correct for the contribution of polarized nitrogen to the longitudinal asymmetry. In the shell model [14], $^{14}$N is described as a spinless $^{12}$C core with the valence proton and neutron being responsible for the nitrogen spin. The correction is expressed [8, 9] in terms of a parametrization of the measured deuteron asymmetry $A_1^{\rm d}$ from Ref.s [15, 16]. This correction is found to be less than 3% of $A_{\parallel}^{\rm p}$ and introduces a small systematic uncertainty.

Our analysis is limited to the kinematic region with $x \geq 0.0008$ and $Q^2 \geq 0.2$ GeV$^2$. Cuts are applied to restrict the inelasticity to $y \leq 0.9$, the scattering angle to $\Theta \geq 2$ mrad, the energy of the scattered muon to $E'_\mu \geq 19$ GeV, and the energy transfer to the target to $\nu \geq 15$ GeV. After these cuts $12.5 \times 10^6$ events from the 1996 measurement remain for the final analysis.

The new results are in agreement with the 1993 data within the statistical errors so we combine them in the subsequent analysis. The combined results for $A_1^{\rm p}$ are given as a function of $x$ and $Q^2$ in Table 1 and shown in Fig. 1. In this figure, we also compare our results and those of EMC [10] to the E143 [17] measurements which are at lower $Q^2$. No evidence for a $Q^2$ dependence of $A_1$ is visible within the accuracy of the present data. Figure 2 shows $A_1^{\rm p}$ as a function of $x$ averaged over $Q^2$ within each $x$ bin. The new results are compared to our 1993 results in Fig. 2(a) and the combined results are shown in Fig. 2(b) along with EMC and E143 data. Our dominant systematic errors at low $x$ are

due to radiative corrections, time-dependence of the acceptance ratio $r$ for events from the upstream and the downstream target cells and uncertainties in $A_2^p$. At high $x$, the dominant sources of systematic errors are uncertainties in the ratio $R$ and in the beam and target polarizations. Individual systematic errors are added in quadrature to obtain the total systematic error.

We compute $g_1^p$ for data with $Q^2 \geq 1$ GeV$^2$ using Eq. (2) and parametrizations for $F_2^p$ and $R$. In our previous publications we used for $F_2^p$ the parametrization provided by the NMC collaboration [18]. Recently, new $F_2^p$ data at lower $x$ became available from NMC [19], E665 [20], H1 [21] and ZEUS [22]. We performed a new fit of $F_2^p$ which includes these new data, the data from SLAC [23], NMC [18] and BCDMS [24], and covers the kinematic range $3.5 \times 10^{-5} < x < 0.85$ and $0.2 < Q^2 < 5000$ GeV$^2$. We use the same functional form as used by NMC [18]

$$F_2(x,Q^2) = A(x) \cdot \left[\frac{\ln(Q^2/\Lambda^2)}{\ln(Q_0^2/\Lambda^2)}\right]^{B(x)} \cdot \left[1 + \frac{C(x)}{Q^2}\right], \qquad (4)$$

where

$$\begin{aligned} A(x) &= x^{a_1}(1-x)^{a_2}\left[a_3 + a_4(1-x) + a_5(1-x)^2 + a_6(1-x)^3 + a_7(1-x)^4\right], \\ B(x) &= b_1 + b_2 x + \frac{b_3}{(x+b_4)}, \\ C(x) &= c_1 x + c_2 x^2 + c_3 x^3 + c_4 x^4, \end{aligned}$$

with $\Lambda = 250$ MeV and $Q_0^2 = 20$ GeV$^2$. In the minimization procedure, the data points were weighted by their statistical errors. The normalization uncertainties and the systematic errors were accounted for by additional parameters in the fit. The resulting fit parameters of $F_2$ are presented in Table 2. This parametrization of $F_2$ has to be used with consistent values of $R$ such that the measured cross sections are reproduced. For $x < 0.12$ we use a parametrization of $R$ measured by the NMC [19]. In the high $x$ region we use the SLAC parametrization for $R$ [25] as in our previous publications.

Figure 3(a) shows $g_1^p$ calculated from our 1996 data using the two sets of $F_2$ and $R$ parametrizations. The resulting differences in the values of $g_1^p$ are small. In the subsequent analysis, we use the new set of parametrizations. The results for $g_1^p(x)$ at the average $Q^2$ of each bin in $x$ for 1996 data are compared to our 1993 data in Fig. 3(b). The old and the new results are statistically compatible; however, the lowest $x$ point in the new data has a lower value. The combined results are shown in the same figure and are listed in Table 3. The data do not suggest a rise of $g_1^p(x)$ at low $x$.

We use our data in the kinematic region $Q^2 \geq 1$ GeV$^2$, $x \geq 0.003$ to evaluate $\Gamma_1^p = \int_0^1 g_1^p(x)\mathrm{d}x$ at a fixed $Q^2$. The precision of the data and the available $Q^2$ range do not allow a direct determination of the $Q^2$ dependence of $A_1^p$ ($\sim g_1/F_1$). Different $Q^2$ behaviours of $g_1$ and $F_1$ are expected from perturbative QCD [2]. The $Q^2$ dependence of $g_1$ is then estimated from a perturbative QCD analysis in NLO in the Adler-Bardeen scheme [2] as performed in our previous publications [6, 15]. We have updated our analysis to include new published neutron data [26, 27, 28] and our 1996 proton data in addition to the data [6, 10, 15, 16, 17, 29] used in our previous publications. This results in a small change in the QCD fit. The result of the fit for $g_1^p$ is shown in Fig. 4.

Starting from $g_1(x,Q^2)$ at the measured $x$ and $Q^2$ of our experiment we obtain $g_1$ at a fixed $Q_0^2$ as follows:

$$g_1(x,Q_0^2) = g_1(x,Q^2) + [g_1^{\mathrm{fit}}(x,Q_0^2) - g_1^{\mathrm{fit}}(x,Q^2)], \qquad (5)$$

where $g_1^{\rm fit}(x,Q_0^2)$ and $g_1^{\rm fit}(x,Q^2)$ are the values of $g_1$ evaluated at $Q_0^2$ and at the $Q^2$ of the experiment, using the fit parameters. We choose $Q_0^2 = 10\,{\rm GeV}^2$ which is close to the average $Q^2$ of our data. The resulting $g_1$ is given in Table 3.

In the measured range, $0.003 < x < 0.7$, the contribution to the first moment of the proton structure function is

$$\int_{0.003}^{0.7} g_1^{\rm p}(x,Q_0^2)dx = 0.139 \pm 0.006 \pm 0.008 \pm 0.006 \quad (Q_0^2 = 10\ {\rm GeV}^2), \tag{6}$$

where the first uncertainty is statistical, the second is systematic and the third is due to the uncertainty in the $Q^2$ evolution. The uncertainties on the integral of $g_1^p$ in the measured range are separated by source in Table 4. In addition to several sources of uncertainty on $A_1^p$ and uncertainties from $F_2^p$ and $R$, contributions due to kinematic smearing and residual biases of the extraction and combination of the asymmetries are also listed. These contributions were studied with Monte Carlo techniques simulating realistic data taking conditions and found to be small. Fig. 5 shows $xg_1^{\rm p}$ as a function of $x$. In this figure the area under the data points represents the integral given in Eq. 6. Evaluating the integral in the measured $x$-region from the QCD fit gives 0.136 which is consistent with Eq. 6.

To estimate the contribution to the first moment from the unmeasured high $x$ region $0.7 < x < 1.0$, we assume $A_1^p = 0.7 \pm 0.3$ which is consistent with the data and covers the upper bound $A_1 \leq 1$. We obtain

$$\int_{0.7}^{1} g_1^{\rm p}(x,Q_0^2)dx = 0.0015 \pm 0.0006. \tag{7}$$

To estimate the contribution from the unmeasured low $x$ region we consider two approaches :

1/- Consistent with a Regge behaviour $g_1^{\rm p} \propto x^{-\alpha}$ $(-0.5 \leq \alpha \leq 0.0)$ [30], we assume $g_1^{\rm p}$ = constant at 10 GeV$^2$. This constant, $0.69 \pm 0.14$, obtained from the three lowest $x$ data points evolved to 10 GeV$^2$, leads to

$$\int_{0.0}^{0.003} g_1^{\rm p}(x,Q_0^2)dx = 0.002 \pm 0.002 \quad \text{(Regge assumption)}, \tag{8}$$

where we assign a 100% error to this extrapolation, as was done in our previous publications [5, 6]. The area under the dot-dashed curve in Fig. 5 and its inset corresponds to this low $x$ contribution.

2/- Alternatively, we calculate the low $x$ integral from the QCD fit. Integrating this fit in the low $x$ region gives

$$\int_{0.0}^{0.003} g_1^{\rm p}(x,Q_0^2)dx = -0.011 \pm 0.011 \quad \text{(QCD analysis)}. \tag{9}$$

The area under the QCD fit for $x < 0.003$ in Fig. 5 and its inset corresponds to this low $x$ contribution. The uncertainty in the low $x$ integral is obtained using the same procedure as for the estimation of the uncertainty in the QCD evolution described in [6]. For the low $x$ region, it is dominated by the uncertainties in factorization and renormalization scales.

We note that the two approaches described above lead to different contributions. The inset in Fig. 5 illustrates this difference. The corresponding values for the first moment $\Gamma_1^{\rm p}(Q^2) = \int_0^1 g_1^{\rm p}(x,Q^2)dx$ of $g_1^{\rm p}$ over the entire range in $x$ are,

$$\Gamma_1^{\rm p}(Q_0^2 = 10{\rm GeV}^2) \;=\; 0.142 \pm 0.006 \pm 0.008 \pm 0.006 \quad \text{(Regge)} \tag{10}$$

$$\Gamma_1^p(Q_0^2 = 10\mathrm{GeV}^2) \;=\; 0.130 \pm 0.006 \pm 0.008 \pm 0.014 \quad (\mathrm{QCD}) \tag{11}$$

where the first uncertainty is statistical and the second is systematic. The third uncertainty is due to the low $x$ extrapolation and the $Q^2$ evolution, both of which have theoretical origins, and due to the high $x$ extrapolation. The data do not allow us to exclude either approach so we keep the two numbers using the larger value for the third uncertainty

$$\Gamma_1^p(Q_0^2 = 10\mathrm{GeV}^2) = \left.\begin{array}{c} 0.142\ (\mathrm{Regge}) \\ 0.130\ (\mathrm{QCD}) \end{array}\right\} \pm 0.006 \pm 0.008 \pm 0.014 \tag{12}$$

Assuming $\mathrm{SU}(3)_f$ symmetry within the baryon octet we determine the flavor singlet axial charge $a_0(Q^2) = a_u + a_d + a_s$ of the nucleon using the experimentally determined first moment of the proton and the relation

$$\Gamma_1^p(Q^2) = \frac{C_1^{\mathrm{NS}}(Q^2)}{12}\left[a_3 + \frac{a_8}{3}\right] + \frac{C_1^{\mathrm{S}}(Q^2)}{9} a_0(Q^2). \tag{13}$$

For $a_3 = g_A/g_V = F + D$ and $a_8 = 3F - D$ we take values calculated from the experimental measurements, $g_A/g_V = 1.2601 \pm 0.0025$ [31] and $F/D = 0.575 \pm 0.016$ [32]. For the singlet and non-singlet coefficient functions $C_1^{\mathrm{S}}$ and $C_1^{\mathrm{NS}}$ we use values calculated to 3rd order in $\alpha_s$ [33]. Using the relations $a_8 = a_u + a_d - 2a_s$ and $a_3 = a_u - a_d$ we can calculate the individual quark flavor matrix elements. Results based on our proton data are given in Table 5. Assuming $\mathrm{SU}(3)_f$ and $a_s = 0$, Ellis and Jaffe predicted a sum rule which gives for the above given couplings a theoretical value of $\Gamma_1^p = 0.170 \pm 0.004$ [34]. Irrespective of whether we take the Regge or the QCD approach in the low $x$ region our result for the first moment $\Gamma_1^p$ is smaller than the Ellis-Jaffe prediction and our value of $a_s$ is negative. The more conservative estimate of the uncertainty in the low $x$ extrapolation results in the increase of uncertainties shown in Table 5 compared to our previous publications.

In the naive QPM the axial coupling $a_0(Q^2)$ is identified with $\Delta\Sigma$, the quark spin contribution to the nucleon spin. In the QCD improved QPM because of the U(1) anomaly there is a contribution of the gluon spin to $a_0(Q^2)$ which makes $\Delta\Sigma$ strongly scheme dependent. In the Adler-Bardeen scheme used in our QCD analysis, $a_0(Q^2)$ is decomposed into quark and gluon contributions in the following way

$$a_0(Q^2) = \Delta\Sigma - n_f \frac{\alpha_s(Q^2)}{2\pi} \Delta g(Q^2), \tag{14}$$

where $\Delta g$ is the gluon spin contribution to the nucleon spin. In this decomposition $\Delta\Sigma$ is $Q^2$ independent which enables it to be interpreted as the intrinsic quark-spin content of the nucleon. When we make the assumption $\Delta\Sigma = a_8$ corresponding to an unpolarized strange sea, our measurement of $a_0$ corresponds to $2 < \Delta g < 3$ at $Q^2 = 10$ GeV$^2$.

The QCD analysis done with all the published data along with the data presented in this paper results in $\Delta g = 0.9 \pm 0.3(\mathrm{exp}) \pm 1.0(\mathrm{theory})$ at $Q^2 = 1$ GeV$^2$ and the corresponding value of $\Delta g$ at $Q^2 = 10$ GeV$^2$ is 1.7.

In ref. [15] we have presented $\Gamma_1^d$ using the Regge extrapolation approach for the unmeasured low $x$ region. This is similar to the approach leading to Eq. (10). Combining the result from Eq. (10) with $\Gamma_1^d = 0.041 \pm 0.008$ at $Q_0^2 = 10$ GeV$^2$ [15] we obtain for the Bjorken sum

$$\Gamma_1^p - \Gamma_1^n = 0.195 \pm 0.029 \quad (\mathrm{Q}_0^2 = 10\ \mathrm{GeV}^2). \tag{15}$$

which agrees with the theoretical prediction at $Q_0^2 = 10$ GeV$^2$

$$\Gamma_1^p - \Gamma_1^n = \frac{1}{6}\left|\frac{g_A}{g_V}\right| C_1^{NS} = 0.186 \pm 0.003 \quad (Q_0^2 = 10 \text{ GeV}^2). \tag{16}$$

This conclusion is obviously unchanged if we use the result from the Regge extrapolation with an enlarged error from Eq. (12).

An alternative test of the Bjorken sum rule using QCD has been performed [35], which uses a QCD fit leaving $g_A/g_V$ free, whereas $g_A/g_V$ is held fixed in our fit.

In summary, we present a new measurement of the spin-dependent structure function of the proton, $g_1^p(x,Q^2)$, from polarized deep inelastic muon proton scattering. The new results are in agreement with our previous data and the statistical errors are reduced by a factor of 2. They do not confirm an earlier indication of a possible rise of $g_1^p(x)$ at low $x$. The reduction of the statistical error is not reflected in the final error on the first moment $\Gamma_1^p$ because the uncertainty in the low $x$ extrapolation has been enlarged in view of recent theoretical developments. This uncertainty which is now the dominant source of error in $\Gamma_1^p$ can only be reduced significantly by future measurements [36] of the structure function in the very low $x$ region. Such uncertainties however do not prevent us from confirming the violation of the Ellis-Jaffe sum rule. Combining the new value for $\Gamma_1^p$ with our published $\Gamma_1^d$ confirms the Bjorken sum rule with an accuracy of 15% at the one standard deviation level. Large uncertainties in the estimation of $\Delta g$ from the QCD analysis exist at present due to the theoretical uncertainties. This points to the need of direct measurements [37] of $\Delta g$ through processes in which the gluon polarization contributes at leading order.

## References


[1] J.D. Bjorken, Phys. Rev. 148 (1966) 1467; Phys. Rev. D1 (1970) 1376.
[2] R. D. Ball, S. Forte, and G. Ridolfi, Phys. Lett. B378 (1996) 255.
[3] M. Glück et al., Phys Rev. D53 (1996) 4775.
[4] T. Gehrmann and W.J. Stirling, Phys. Rev. D53 (1996) 6100.
[5] SMC, D. Adams et al., Phys. Lett. B329 (1994) 399.
[6] SMC, D. Adams et al., *Spin Structure of the Proton from Polarized Deep Inelastic Muon-Proton Scattering*, accepted for publication in Phys. Rev. D. (CERN-PPE/97-22)
[7] P. Schüler, Proc. 8th Int. Symposium on High Energy Spin Physics, Minneapolis 1988, ed. by K.J. Heller, AIP Conference Proceedings Vol. 187; E. Burtin Docteur en Sciences thesis, University of Paris-Sud, July 11, 1996
[8] SMC, B. Adeva et al., Submitted to Nuclear Instrument Methods A. (CERN-PPE/97-66)
[9] M. Borghini, in Proc. 2nd Int. Conf. on Polarized Targets, Berkeley, 1971, ed. by G. Shapiro.
[10] EMC, J. Ashman et al., Phys. Lett. B206 (1988) 364; Nucl. Phys. B328 (1989) 1.
[11] V. W. Hughes and J. Kuti, Ann. Rev. Nucl. Part. Sci. 33 (1983) 611; T. Pussieux and R. Windmolders, in: *Internal Spin Structure of the Nucleon*, ed. by V.W. Hughes and C. Cavata (World Scientific, Singapore, 1995), p. 212.
[12] SMC, D. Adams et al., Phys. Lett. B336 (1994) 125.
[13] E143 Collaboration, K. Abe et al., Phys. Rev. Lett. 76 (1996) 587.
[14] J. M. Blatt and V. F. Weisskopf, *Theoretical Nuclear Physics* (Dover Publications Inc., New York, 1979)

[15] SMC, D. Adams et al., Phys. Lett. B396 (1997) 338.
[16] E143 Collaboration, K. Abe et al., Phys. Rev. Lett. 75 (1995) 25.
[17] E143 Collaboration, K. Abe et al., Phys. Rev. Lett. 74 (1995) 346.
[18] NMC, M. Arneodo et al., Phys. Lett. B364 (1995) 107.
[19] NMC, M. Arneodo et al., Nucl. Phys. B483 (1997) 3.
[20] E665 Collaboration, M.R. Adams et al., Phys. Rev. D54 (1996) 3006.
[21] H1 Collaboration, S. Aid et al., Nucl. Phys. B470 (1996) 3.
[22] ZEUS Collaboration, M. Derrick et al., Z. Phys. C72 (1996) 399.
[23] SLAC, L. W. Whitlow et al., Phys. Lett. B282(1992) 475.
[24] BCDMS Collaboration, A.C. Benvenuti et al., Phys. Lett. B233 (1989) 485.
[25] SLAC, L.W. Whitlow et al., Phys. Lett. B250 (1990) 193.
[26] E142 Collaboration, P.L. Anthony et al., Phys. Rev. Lett. 71 (1993) 959; Phys. Rev. D54 (1996) 6620.
[27] E154 Collaboration, K. Abe et al. SLAC-PUB-7460 (1997) and hep-ex/9705017.
[28] HERMES Collaboration, K. Ackerstaff et al., OAP-741 and hep-ex/9703005.
[29] E143 Collaboration, K. Abe et al., Phys. Lett. B364 (1995) 61.
[30] R. G. Roberts, *The structure of the proton*, Cambridge Monographs on Mathematical Physics (1990).
[31] Particle Data Group, R.M. Barnett et al., Phys. Rev. D54 (1996) 1.
[32] F.E. Close and R.G. Roberts, Phys. Lett. B316 (1993) 165.
[33] S.A. Larin, Phys. Lett. B334 (1994) 192.
[34] J. Ellis and R.L. Jaffe, Phys. Rev. D9 (1974) 1444; *ibid* D10 (1974) 1669.
[35] G. Altarelli et al. Nucl. Phys. B496 (1997) 337.
[36] R. Ball et al., *Future Physics at HERA*, Proceedings of the Workshop 1995/96 ed. by G. Ingelman et al. p. 777.
[37] COMPASS proposal, CERN/SPSLC/P297; A. De Roeck et al., *Future Physics at HERA*, Proceedings of the Workshop 1995/96 ed. by G. Ingelman et al. p. 803; Y. I. Makdisi, Proc. 12th Int. Symposium on High Energy Spin Physics, Amsterdam 1996, ed. by C.W. de Jager et al., (World Scientific, Singapore, 1997), p. 107; V.W. Hughes et al. *ibid* p. 643; SLAC proposal, PROPOSAL-E156.

| $< x >$ | $< Q^2 >$ (GeV$^2$) | $A_1^p$ | $< x >$ | $< Q^2 >$ (GeV$^2$) | $A_1^p$ |
|---|---|---|---|---|---|
| 0.0009 | 0.25 | 0.001 ± 0.069 | 0.0342 | 5.80 | 0.134 ± 0.050 |
| 0.0011 | 0.30 | 0.016 ± 0.085 | 0.0344 | 7.77 | 0.032 ± 0.035 |
| 0.0011 | 0.34 | 0.196 ± 0.111 | 0.0359 | 10.14 | 0.082 ± 0.041 |
| 0.0014 | 0.38 | 0.139 ± 0.044 | 0.0472 | 4.29 | 0.054 ± 0.108 |
| 0.0017 | 0.46 | 0.076 ± 0.053 | 0.0473 | 5.86 | 0.084 ± 0.068 |
| 0.0019 | 0.55 | 0.037 ± 0.057 | 0.0479 | 7.83 | 0.103 ± 0.040 |
| 0.0023 | 0.58 | 0.020 ± 0.040 | 0.0485 | 10.95 | 0.120 ± 0.029 |
| 0.0025 | 0.70 | 0.025 ± 0.044 | 0.0527 | 14.72 | 0.133 ± 0.042 |
| 0.0028 | 0.82 | 0.027 ± 0.048 | 0.0736 | 5.47 | 0.145 ± 0.101 |
| 0.0035 | 0.88 | 0.038 ± 0.029 | 0.0744 | 7.88 | 0.153 ± 0.059 |
| 0.0043 | 1.14 | -0.011 ± 0.025 | 0.0750 | 11.08 | 0.196 ± 0.037 |
| 0.0051 | 1.43 | 0.060 ± 0.030 | 0.0762 | 16.30 | 0.170 ± 0.029 |
| 0.0056 | 1.71 | 0.008 ± 0.051 | 0.0855 | 23.05 | 0.189 ± 0.045 |
| 0.0069 | 1.43 | -0.003 ± 0.043 | 0.1189 | 7.41 | 0.368 ± 0.104 |
| 0.0072 | 1.76 | 0.016 ± 0.033 | 0.1196 | 11.14 | 0.335 ± 0.068 |
| 0.0077 | 2.04 | 0.063 ± 0.032 | 0.1200 | 16.48 | 0.245 ± 0.048 |
| 0.0084 | 2.34 | 0.105 ± 0.037 | 0.1206 | 24.82 | 0.248 ± 0.043 |
| 0.0090 | 2.63 | 0.099 ± 0.048 | 0.1293 | 34.32 | 0.264 ± 0.060 |
| 0.0095 | 2.94 | -0.041 ± 0.072 | 0.1711 | 10.19 | 0.203 ± 0.102 |
| 0.0114 | 1.75 | -0.075 ± 0.110 | 0.1715 | 16.51 | 0.293 ± 0.080 |
| 0.0120 | 2.07 | 0.065 ± 0.072 | 0.1717 | 24.89 | 0.214 ± 0.068 |
| 0.0124 | 2.36 | 0.032 ± 0.054 | 0.1718 | 34.94 | 0.459 ± 0.073 |
| 0.0125 | 2.66 | 0.017 ± 0.045 | 0.1771 | 45.48 | 0.361 ± 0.081 |
| 0.0127 | 2.96 | -0.014 ± 0.039 | 0.2368 | 10.54 | 0.363 ± 0.132 |
| 0.0133 | 3.30 | 0.008 ± 0.033 | 0.2389 | 16.54 | 0.146 ± 0.096 |
| 0.0147 | 3.74 | 0.046 ± 0.032 | 0.2394 | 24.95 | 0.424 ± 0.081 |
| 0.0165 | 4.43 | 0.112 ± 0.029 | 0.2398 | 34.94 | 0.426 ± 0.084 |
| 0.0184 | 5.44 | -0.029 ± 0.047 | 0.2462 | 52.74 | 0.471 ± 0.057 |
| 0.0231 | 2.78 | 0.142 ± 0.111 | 0.3388 | 15.26 | 0.514 ± 0.158 |
| 0.0236 | 3.31 | 0.227 ± 0.107 | 0.3404 | 25.01 | 0.535 ± 0.149 |
| 0.0235 | 3.77 | -0.030 ± 0.077 | 0.3407 | 34.96 | 0.715 ± 0.153 |
| 0.0237 | 4.54 | 0.083 ± 0.041 | 0.3436 | 61.81 | 0.555 ± 0.078 |
| 0.0241 | 5.75 | 0.068 ± 0.030 | 0.4688 | 21.86 | 0.972 ± 0.179 |
| 0.0263 | 7.42 | 0.024 ± 0.034 | 0.4751 | 34.98 | 0.433 ± 0.230 |
| 0.0339 | 4.23 | 0.058 ± 0.073 | 0.4842 | 72.07 | 0.616 ± 0.096 |

Table 1: The virtual photon proton asymmetries $A_1^p$ for different $x$ and $Q^2$ values, with their statistical errors.

| Parameter | Central value | Upper limit | Lower limit |
|---|---|---|---|
| $a_1$ | -0.24997 | -0.24810 | -0.25196 |
| $a_2$ | 2.39635 | 2.36324 | 2.42968 |
| $a_3$ | 0.22896 | 0.23643 | 0.21913 |
| $a_4$ | 0.08498 | -0.03241 | 0.21630 |
| $a_5$ | 3.86079 | 4.22681 | 3.46446 |
| $a_6$ | -7.41428 | -7.81197 | -6.98874 |
| $a_7$ | 3.43422 | 3.58225 | 3.27710 |
| $b_1$ | 0.11411 | 0.09734 | 0.13074 |
| $b_2$ | -2.23556 | -2.22540 | -2.24648 |
| $b_3$ | 0.03115 | 0.03239 | 0.02995 |
| $b_4$ | 0.02135 | 0.02233 | 0.02039 |
| $c_1$ | -1.45174 | -1.43613 | -1.47152 |
| $c_2$ | 8.47455 | 8.10840 | 8.91079 |
| $c_3$ | -34.3791 | -33.3057 | -35.7143 |
| $c_4$ | 45.8881 | 44.7175 | 47.3385 |

Table 2: Values of the fitted parameters for the $F_2$ function given in Eq. (4). In the second column we give the parameters for the central value of the fit, parametrizations for an upper and a lower limit for $F_2$ are given in the last two columns.

| $x$ Range | $\langle x \rangle$ | $\langle Q^2 \rangle$ | $A_1^p$ | $g_1^p$ | $g_1(Q_0^2{=}10.\mathrm{GeV}^2)$ |
|---|---|---|---|---|---|
| 0.003–0.006 | 0.005 | 1.3 | 0.017±0.018±0.003 | 0.44±0.46±0.08 | 0.73±0.46±0.08±0.71 |
| 0.006–0.010 | 0.008 | 2.1 | 0.047±0.016±0.004 | 0.86±0.30±0.07 | 1.12±0.30±0.07±0.26 |
| 0.010–0.020 | 0.014 | 3.6 | 0.035±0.014±0.003 | 0.41±0.16±0.04 | 0.56±0.16±0.04±0.09 |
| 0.020–0.030 | 0.025 | 5.7 | 0.058±0.018±0.005 | 0.43±0.14±0.03 | 0.50±0.14±0.03±0.02 |
| 0.030–0.040 | 0.035 | 7.8 | 0.067±0.022±0.005 | 0.36±0.12±0.02 | 0.38±0.12±0.02±0.01 |
| 0.040–0.060 | 0.049 | 10.4 | 0.115±0.019±0.008 | 0.44±0.07±0.03 | 0.44±0.07±0.03±0.00 |
| 0.060–0.100 | 0.077 | 14.9 | 0.176±0.019±0.013 | 0.42±0.05±0.02 | 0.40±0.05±0.02±0.00 |
| 0.100–0.150 | 0.122 | 21.3 | 0.267±0.025±0.018 | 0.37±0.04±0.02 | 0.35±0.04±0.02±0.00 |
| 0.150–0.200 | 0.173 | 27.8 | 0.318±0.035±0.021 | 0.30±0.03±0.02 | 0.28±0.03±0.02±0.01 |
| 0.200–0.300 | 0.242 | 35.6 | 0.400±0.036±0.028 | 0.23±0.02±0.01 | 0.23±0.02±0.01±0.01 |
| 0.300–0.400 | 0.342 | 45.9 | 0.568±0.058±0.042 | 0.17±0.02±0.01 | 0.19±0.02±0.01±0.01 |
| 0.400–0.700 | 0.480 | 58.0 | 0.658±0.079±0.055 | 0.08±0.01±0.01 | 0.09±0.01±0.01±0.01 |

Table 3: The virtual photon proton asymmetry $A_1^p$, the spin-dependent structure function $g_1^p(x)$ at the measured $Q^2$ and $g_1^p(x)$ evolved to $Q_0^2 = 10$ GeV$^2$. The first error is statistical and the second is systematic. In the last column, the third error indicates the uncertainty in the QCD evolution.

| Source of the error | $\Delta\Gamma_1(0.003 \to 0.7)$ |
|---|---|
| Beam polarization | 0.0052 |
| Target polarization | 0.0039 |
| Dilution factor | 0.0029 |
| Uncertainty on $F_2$ | 0.0025 |
| Acceptance variation | 0.0016 |
| Radiative corrections | 0.0007 |
| Asymmetry extraction | 0.0006 |
| Polarized background | 0.0005 |
| Neglect of $A_2$ | 0.0005 |
| Kinematic resolution | 0.0003 |
| Momentum measurement | 0.0003 |
| Uncertainty on $R$ | 0.0001 |
| Total systematic error | 0.0078 |
| Evolution | 0.0060 |
| Statistics | 0.0056 |

Table 4: The sources of uncertainties in the integral of $g_1^{\mathrm{p}}$ in the measured range $0.003 < x < 0.7$.

| Quantity | SMC Results | |
|---|---|---|
| | Regge approach | QCD approach |
| $\Gamma_1^{\mathrm{p}}$ | $0.142 \pm 0.017$ | $0.130 \pm 0.017$ |
| $a_0$ | $0.34 \pm 0.17$ | $0.22 \pm 0.17$ |
| $a_u$ | $0.84 \pm 0.06$ | $0.80 \pm 0.06$ |
| $a_d$ | $-0.42 \pm 0.06$ | $-0.46 \pm 0.06$ |
| $a_s$ | $-0.08 \pm 0.06$ | $-0.12 \pm 0.06$ |

Table 5: Results for the first moment and the axial charges at $Q^2 = 10$ GeV$^2$ from our proton data.

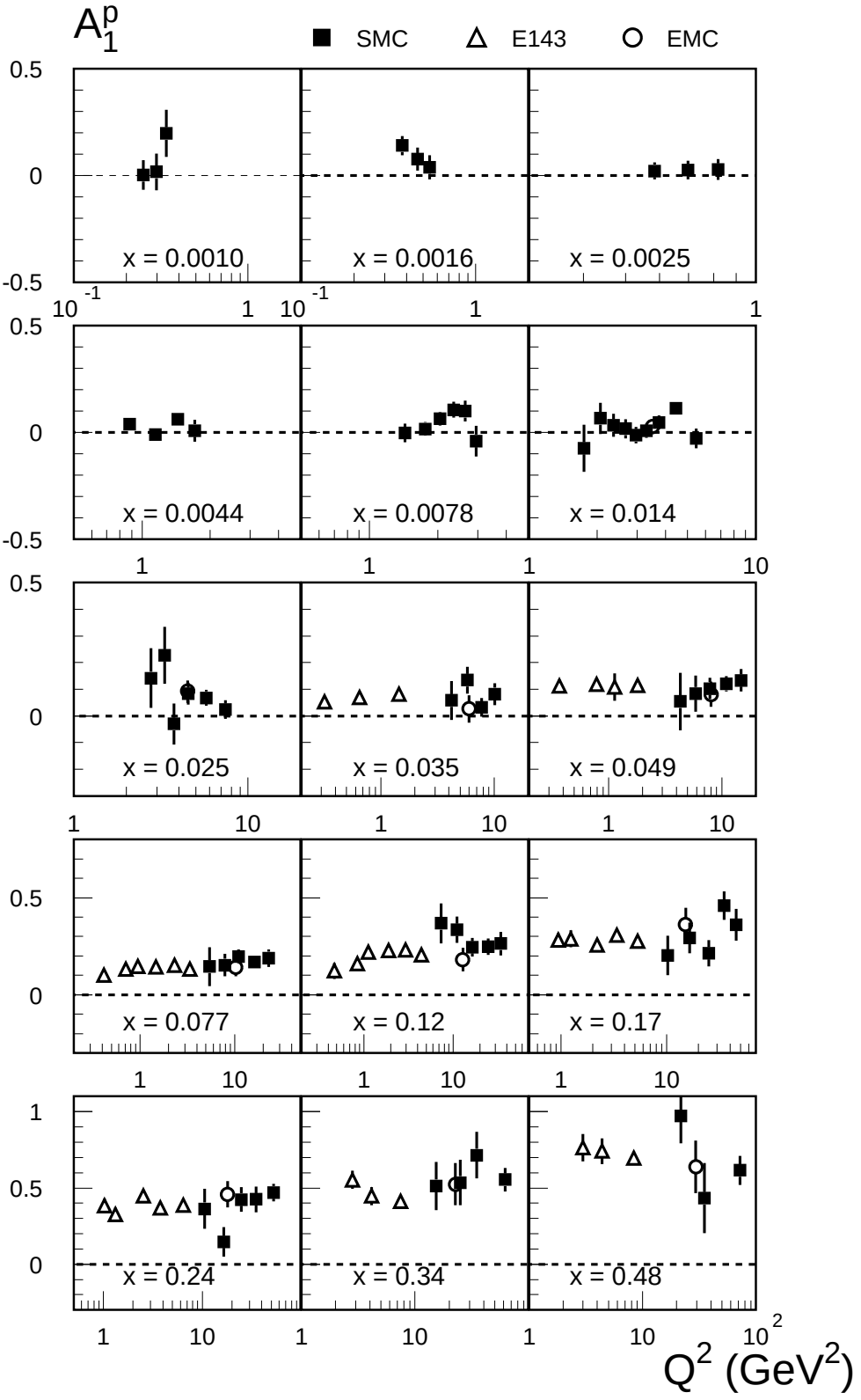


Figure 1: $A_1^p$ vs $Q^2$ for different bins of $x$ for the combined, 1993 and 1996, SMC data (squares) where the value of $x$ corresponds to the average in each bin. At higher $x$ values E143 (open triangles) and EMC (open circles) measurements are shown for comparison. Error bars represent statistical uncertainties.

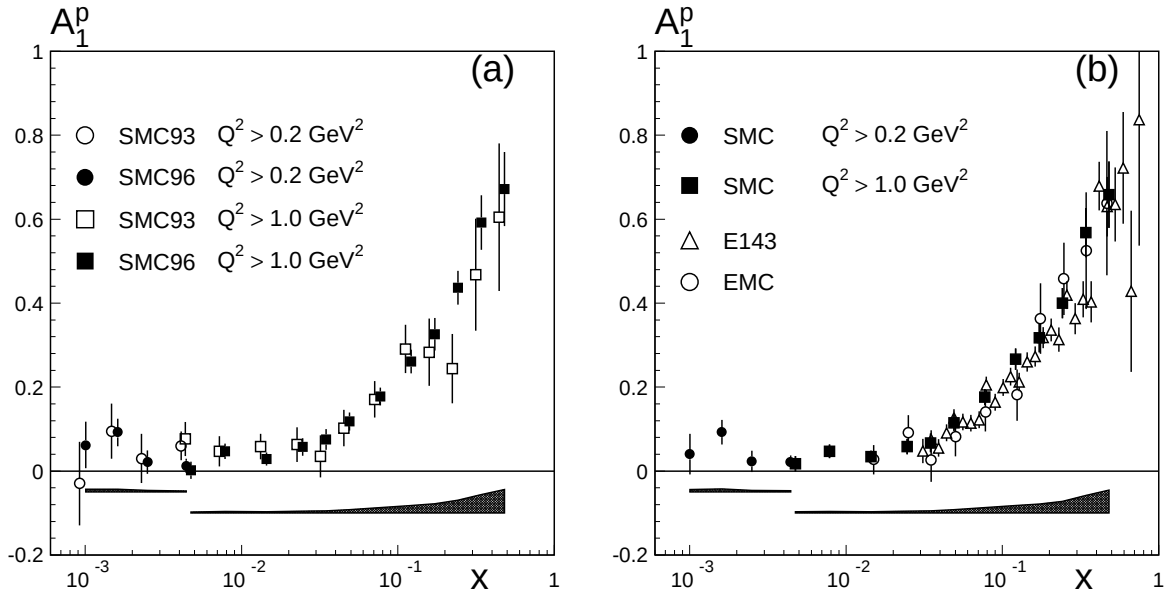


Figure 2: (a) Comparison of $A_1^{\rm p}$ vs $x$ for 1993 and 1996 SMC data at the measured $Q^2$. (b) $A_1^{\rm p}$ vs $x$ from 1993 and 1996 SMC data combined is shown along with the measurements from EMC and E143 experiments. Statistical errors are shown as error bars while the shaded band below indicates the SMC systematic uncertainty.

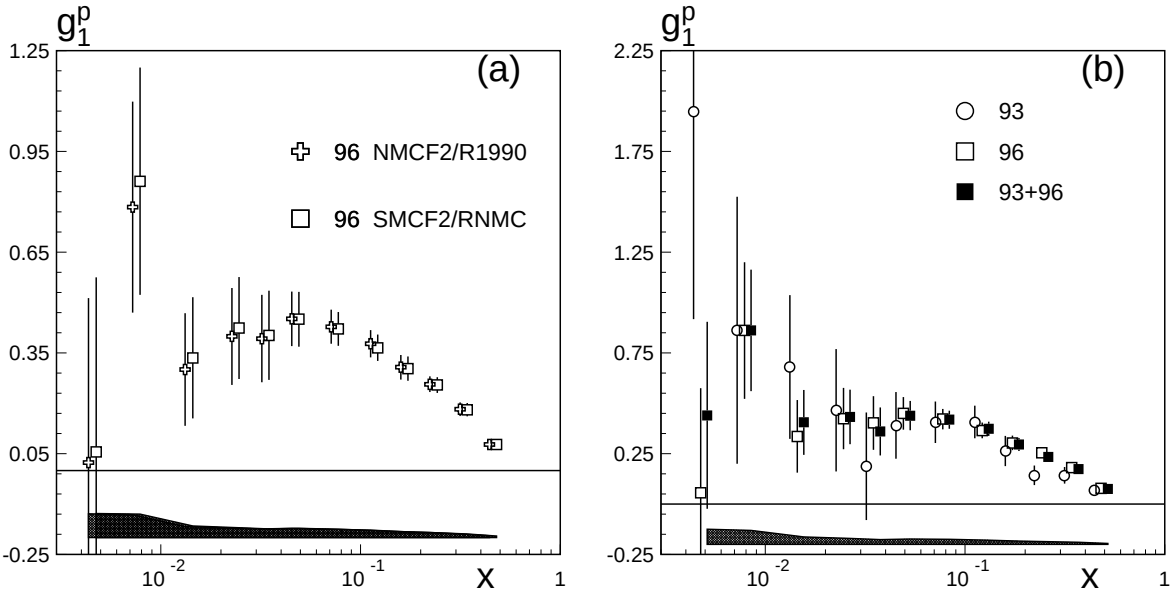


Figure 3: (a) A comparison of $g_1^{\rm p}$ at measured $Q^2$ from 1996 SMC data using the old and the new set of $F_2^{\rm p}$ and $R$ parameterizations (see text). (b) SMC $g_1^{\rm p}$ values at measured $Q^2$ from 1993, 1996 and 1993+1996 combined data sets. In both figures error bars show the statistical uncertainty and the shaded band indicates the systematic uncertainty.

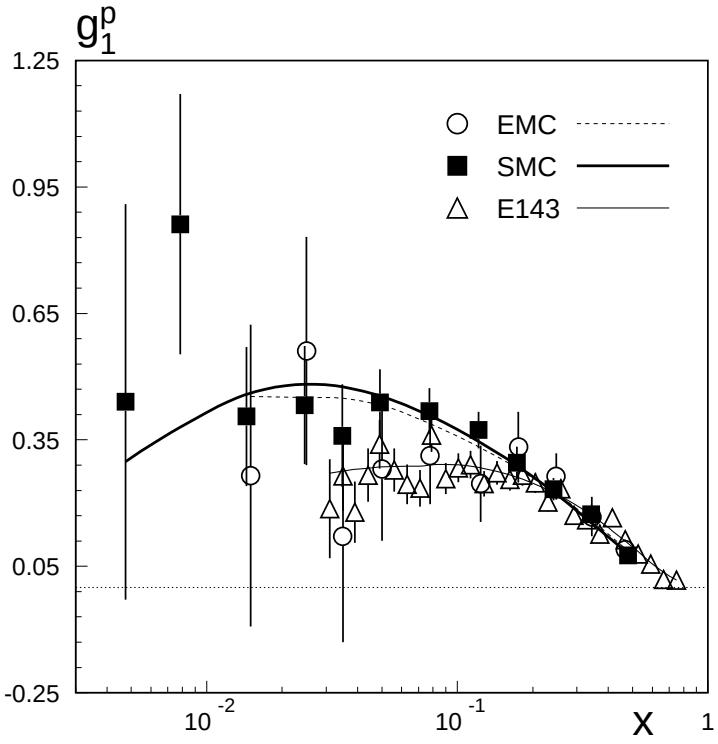


Figure 4: Published data sets on $g_1^p$ are shown. The curves represent the QCD fit at the measured $Q^2$ for each data set. Error bars represent the total error.

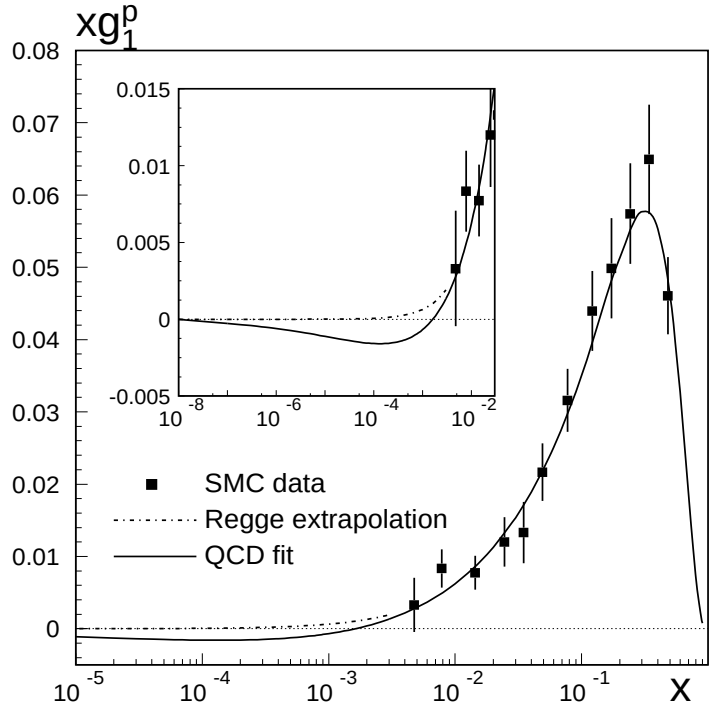


Figure 5: $xg_1^p$ as a function of $x$; SMC data points (squares) with the total error are shown together with the result of the QCD fit (continuous line), both at $Q^2 = 10$ GeV$^2$. For $x < 0.003$ the extrapolation assuming Regge behaviour is indicated by the dot-dashed line. The inset is a close-up extending to lower $x$.